Structure-Function Study on a *de Novo* Synthetic Hydrophobic Ion Channel

Zhi Qi,* Masahiro Sokabe,* Kiyoshi Donowaki,# and Hitoshi Ishida§

*Department of Physiology, Nagoya University School of Medicine, Nagoya, #Department of Molecular Chemistry, Faculty of Engineering, Osaka University, Suita, and §Inoue Photochirogenesis Project, ERATO, Toyonaka, Japan

ABSTRACT Ion conduction properties of a *de novo* synthesized channel, formed from cyclic octa-peptides consisting of four alternate L-alanine (Ala) and *N′*-acylated 3-aminobenzoic acid (Aba) moieties, were studied in bilayer membranes. The single-channel conductance was 9 pS in symmetrical 500 mM KCl. The channel favored permeation of cations over anions with a permeability ratio (P_{Cl^-}/P_{K^+}) of 0.15. The selectivity sequence among monovalent cations based on permeability ratio (P_{X^+}/P_{K^+}) fell into an order: $NH_4^+(1.4) > Cs^+(1.1) \geq K^+(1.0) > Na^+(0.4) \gg Li^+(0)$. The conductance-activity relationship of the channel in K^+ solutions followed simple Michaelis-Menten kinetics with a half-maximal saturating activity of 8 mM and a maximal conductance of 9 pS. The permeability ratio P_{Na^+}/P_{K^+} remained constant (~0.40) under biionic concentrations from 10 to 500 mM. These results suggests that the channel is a one-ion channel. The pore diameter probed by a set of organic cations was ~6 Å. The single-channel current was blocked by Ca^{2+} in a dose-dependent manner that followed a single-site titration curve with a voltage-dependent dissociation constant of 0.6 mM at 100 mV. The electric distance of the binding site for Ca^{2+} was 0.07 from both entrances of the channel, indicating the presence of two symmetrical binding sites in each vicinity of the channel entrance. Correlations between conduction properties and structural aspects of the channel are discussed in terms of a three-barrier and two-binding-site (3B2S) model of Eyring rate theory. All available structural information supported an idea that the channel was formed from a tail-to-tail associated dimer of the molecule, the pore of which was lined with hydrophobic acyl chains. This is the first report to have made a systematic analysis of ion permeation through a hydrophobic pore.

INTRODUCTION

Understanding the physical basis of the structure-function relationship of ion channels is one of the ultimate goals of the study of channels. Many interesting features of ion channels have been unveiled in this decade owing to the development of gene technology and single-channel recording techniques. However, the structural basis of their functions has not been fully understood. The three-dimensional structure of natural channels in the membrane is generally difficult to deduce, even though mutagenesis and expression experiments have provided a great amount of information about functionally important residues and sequence segments (Andersen and Koeppe, 1992). It is a fact that we are at an unbalanced dichotomy between a plethora of high-resolution characterizations of channel functions from single-channel recordings and a dearth of high-resolution structural information. Obviously, it is essential to construct a high-resolution channel structure that can correlate with its function. One way to do so is to take advantage of the simpler structure of the artificial ion channel to build a model channel system. Such model channels have been paid great attention (Sokabe et al., 1997) and developed by means of several different strategies: by employing the channel-forming antibiotics, such as the gramicidin channel (see Andersen and Koeppe, 1992 for review); by mimicking the sequence of the pore region of known channel proteins (Oiki et al., 1988a,b); or by *de novo* design (Lear et al., 1988; Kobuke et al., 1992; Tanaka et al., 1995; Ishida et al., 1997).

Synthetic channel-forming molecules generally have simpler primary structures and fewer atoms, which enable us relatively easily to infer their three-dimensional structures and to do theoretical calculations at the atomic level. Studies on the gramicidin A channel and its analogs have greatly increased our knowledge on the permeation and gating mechanism of ion channels (for review see Andersen and Koeppe, 1992; Roux and Karplus, 1994). Formation of transmembrane ion channels by the peptides, which were synthesized to mimic the sequences of the putative pore-lining segments of the voltage-dependent sodium and acetylcholine receptor channels, gives strong evidence for the pore-forming domain of these channels (Oiki et al., 1988a,b). A K^+-selective channel formed by resorcinol-octadecanal cyclotetramer in planar lipid bilayers (Tanaka et al., 1995) has implied that a cage formed from tetrameric aromatic rings serves as an ion-selective filter for voltage-gated K^+ channels, which gives powerful evidence for the theoretical considerations on the K^+ selectivity of the channels (Heginbotham and MacKinnon, 1992; Miller, 1993).

Analyses of single-channel currents can provide certain information on the channel structure and bridge the gap in understanding the relationship between the molecular structure and function of ion channels (Sokabe et al., 1991). A

Received for publication 16 March 1998 and in final form 16 October 1998.

Address reprint requests to Dr. Masahiro Sokabe, Department of Physiology, Nagoya University School of Medicine, 65 Tsurumai-Cho, Showa-ku, Nagoya, Aichi 466, Japan. Tel.: 81-52-744-2051; Fax: 81-52-744-2057; E-mail: e43429a@nucc.cc.nagoya-u.ac.jp.

0006-3495/99/02/631/11 $2.00

primary purpose of the present work is to construct a structure model of a channel that can correlate with its function. To achieve this aim, a channel formed from cyclo(-Ala-Aba(C_{16})-)$_4$ (AC164), a cyclic octa-peptide consisting of four alternate L-alanine (Ala) and *N′*-acylated 3-aminobenzoic acid (Aba) moieties (Ishida et al., 1997), was studied in bilayer membranes. The function and structure of the channel to provide a conduction pathway for permeant ions was studied by electrophysiological experiments. Correlations between them were further analyzed in terms of a three-barrier and two-binding-site (3B2S) model of Eyring rate theory. From all available structural information, it is difficult to escape a conclusion that the channel is formed from a tail-to-tail associated dimer of the cyclic peptide, in which the pore is lined with hydrophobic acyl chains. As a result, this channel can provide a good model for further study of solving an intriguing problem that the pore regions of some natural channel proteins are surprisingly hydrophobic in comparison with what might have been expected for cation channels (Kumpf and Dougherty, 1993). For example, 19 residues . . . MTLSISVLLSLTVFLLVIV. . . in each of the M2 segments of the nicotinic acetylcholine receptor (nAChR), which are supposed to form a part of the pore lining, are uncharged and mostly hydrophobic (for review see Karlin and Akabas, 1995). Similarly, in the shaker K^+ channel, the putative pore-forming segment is predominantly nonpolar residues (Tempel et al., 1987). Thus, insight into the mechanism of how an ion can permeate through the AC164 channel is applicable to that in hydrophobic pore regions of natural channels.

The proposed structure of the pore in this study challenges the conventional belief that a pore of an ion channel should be lined with charged or polar residues to alternatively replace the solvation structure of the permeant ion (Jordan, 1990). Some preliminary results have appeared elsewhere (Sokabe et al., 1996).

MATERIALS AND METHODS

Synthesis of the AC164 molecule

The AC164 molecule, which was designed to act as a half-pore, was synthesized by the stepwise coupling and cyclization of the component dipeptides on an oxime resin. As the detailed synthetic process will be described elsewhere (Sokabe, Z. Q., M. Sokabe, K. Donowaki, Y. Inoue, and H. Ishida, manuscript in preparation), only a brief explanation will be made here. First, palmitic acid (C_{16}) was condensed with 3-(*N-tert*-butoxycarbonylamino)-5-aminobenzoic acid ethyl ester, Boc-Daba(H)-OEt using dicyclohexylcarbodiimide (DCC) and 1-hydrozybenzotriazole (HOBt), to produce the *N*-Boc-protected and *N′*-acylated compound, Boc-Daba(C_{16})-OEt. The *N*-Boc group was then removed by treatment with trifluoroacetic acid (TFA), and the resultant amine coupled with Boc-Ala-OH to yield the dipeptide, Boc-Ala-Daba(C_{16})-OEt, again using DCC-HOBt coupling methodology. Subsequently, Boc-Ala-Daba(C_{16})-OH was prepared by stirring the ethyl ester in 1 N NaOH. In readiness for the solid-phase synthesis, Boc-Ala-Daba(C_{16})-OH was attached to the resin using DCC in CH_2Cl_2. This was followed by the stepwise coupling of the second, third, and fourth dipeptides, in each case using [(benzotriazol-1-yl)oxy]tris(dimethylamino)-phosphonium hexa-fluorophosphate (BOP) and HOBt in *N,N*-dimethylformamide (DMF). Cyclization was performed on the resin. Initial treatment with 25% TFA-CH_2Cl_2 removed the *N*-Boc group, and the subsequent treatment with a DMF solution containing acetic acid (2 mol Eq with respect to the octapeptide) and triethylamine (2 Eq) afforded the target cyclic peptide, AC164,

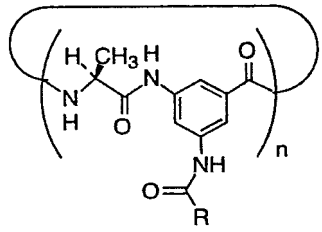

where $n = 4$ and R = $C_{15}H_{31}$. One of its component is shown by a stick model in Fig. 1 *A*. The ^{1}H-NMR and mass spectral data are shown below. As no signals for impurities are observed in the ^{1}H-NMR spectrum, the purity of the compound may be assigned as greater than 99%. ^{1}H-NMR (DMSO-δ_6) δ 10.33–10.01(8H, multiplet, 3, 5-amide), 8.48–8.27(4H, multiplet, amide(Ala)), 8.19–7.58(12H, multiplet, 2, 4, 6-phenyl), 4.70–4.53(4H, multiplet, αCH), 2.33–2.29(8H, multiplet, 2-acyl), 1.59(8H, broad, 3-acyl), 1.43(12H, broad, βCH_3), 1.25(96H, broad, 4–15-acyl), 0.83(12H, triplet, 16-acyl); ^{13}C NMR (DMSO-d_6) δ 171.6 (8C, C = O(Ala and acyl)), 166.6 (4C, C = O(aminobenzoate)), 139.7 (4C, 3-phenyl), 139.2 (4C, 5-phenyl), 135.6 (4C, 1-phenyl), 113.6 (4C, 2-phenyl), 113.2 (4C, 4-phenyl), 112.7 (4C, 6-phenyl), 50.0 (4C, α-CH(Ala)), 38.9 (4C, 2-acyl), 31.3 (4C, 3-acyl), 29.0 (40C, 4–13-acyl), 25.1 (4C, 14-acyl), 22.1 (4C, 15-acyl), 17.6 (4C, CH_3(acyl)), 13.9 (4C, β-CH_3(Ala)); MS mass to charge ratio calculated for (M + Na) $C_{104}H_{164}O_{12}N_{12}$ 1797.5, found 1797.1.

Molecular modeling

A structural model of the channel was constructed on a Silicon Graphics Indigo2 workstation by using Insight II 95 and Discover 95 (Biosym/MSI, San Diego, CA) programs as previously described (Qi and Sokabe, 1998). A primitive structure of the AC164 molecule was built according to its one-dimensional sequence, using a configuration with an exact four-fold rotational symmetry. An initial conformation was then obtained using a modified, flat-bottomed function that rendered the cavity so small that it simply expanded only in the subsequent conformational search. During this search, a 100-ps molecular dynamics run of 1-fs time step at 1000 K was employed with harmonic restraints to retain the symmetrical structure. Full conformations generated at 1000 K were placed into five families by creating groups of related structures in which the mutual root mean square deviations were less than a threshold value of 1.6 Å. The average conformation derived from each family was cooled from 1000 K to 300 K at a rate of 7 K per 100 steps. Each conformation was then energy minimized with small restraints to retain the symmetry of the monomer. The monomer with a diameter consistent with the experimental result was produced using the Insight II molecular modeling system (Fig. 1 *D*). A structure of the channel was constructed by connecting two monomers together with a staggered-*trans* configuration, affording a structure that is ~40 Å in length (Fig. 1 *E*); this is the approximate thickness of the lipid bilayer membrane (Egberts et al., 1994).

Bilayer membrane preparation and AC164 channel incorporation

Planar bilayers were formed by applying phosphatidylcholine (PC; asolectin type IV, Sigma Chemical Co., St. Louis, MO) solutions (40 mg/ml in *n*-decane) to a hole (300–500 μm in diameter) in a polypropylene partition separating two solution-filled chambers as described earlier (Nomura et al., 1990). A small aliquot (10–30 μl) of solution containing AC164 molecules (mol wt = 1774.5) dissolved in dimethylsulfoxide (DMSO; Wako Pure Chemical Industries, Ltd., Osaka, Japan) (1 mg/ml, ~0.56 mM) was added to both sides of the preformed bilayer membrane as described elsewhere

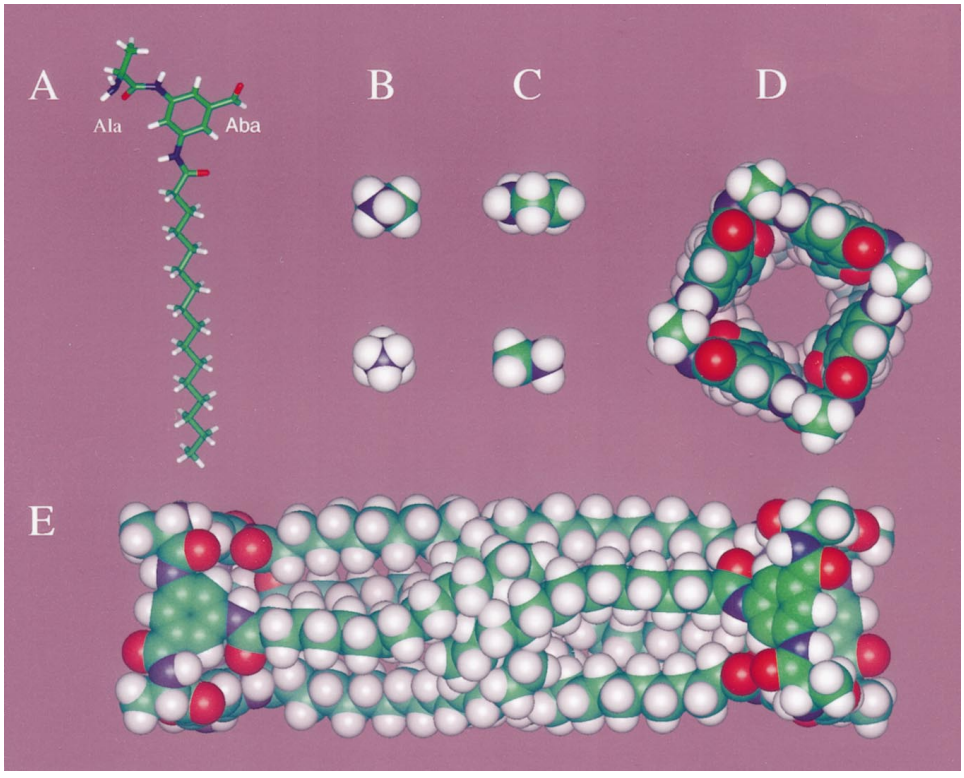

FIGURE 1 (*A*) One component of the AC164 monomer shown by a stick model. Ala, L-alanine; Aba, 3-aminobenzoic acid. (*B* and *C*) CPK models of monomethylammonium and monoethylammonium ions with their biggest (upper) and smallest (lower) section areas. (*D* and *E*) Top and side views of a CPK model of the AC164 channel consisting of a tail-to-tail associated dimer of the AC164 molecule. Color codes: green, carbon; blue, nitrogen; red, oxygen; white, hydrogen.

(Kobuke et al., 1992). Alternatively, a DMSO solution of AC164 was premixed with the phospholipid solution (1:9, v/v) in a tube and was bath sonicated for 1 min to force the AC164 molecule into the lipid solution as much as possible. Several minutes after sonication, the mixed solution automatically separated into two phases, where an *n*-decane solution formed an upper phase and a DMSO solution a lower phase. The bilayer membrane was formed from the *n*-decane solution, into which a certain amount of peptide was expected to move. In either case, AC164 molecules could form an ion channel with the same properties. As the latter method was more successful, we employed it in most of the experiments. The same procedure for the control experiment with DMSO only could not produce channel activity in bilayers. To eliminate the possibility that the channel was formed from some contaminations in a high concentration of the AC164 solution, we gradually lowered the concentration of AC164 in the DMSO solution to 1 μM, but no noticeable difference was observed for the single-channel behaviors. Curiously, the success rate of channel formation was only slightly improved by the high concentration of the AC164. Due to its poor solubility in the lipid phase, it is suspected that most of the AC164 molecules form an aggregation in the lipid solution such that they cannot participate in the formation of an ion channel. However, we used higher concentrations in most experiments to improve the success rate as much as possible.

Transmembrane currents through voltage-clamped bilayers were low-pass filtered at 10 kHz through a bilayer-clamp amplifier (model BC-525C, Warner Instrument Co., Hamden, CT) and recorded on a magnetic tape by means of a PCM recorder (VR-10B, Instrutech Co.). The side to which lipid solution was smeared was defined as *cis*. The opposite side, which was connected to the signal ground of the amplifier, was defined as *trans*. The voltage was referred to the *cis* side with respect to the *trans* side. All solutions used were buffered by 5 mM HEPES and adjusted with Tris base to pH 7.2. Organic cations used to probe the size of the channel pore were of special grade and obtained from the following chloride salts: ammonium, monomethylammonium, monoethylammonium, aminoguanidinium, diethylammonium, choline, tetramethylammonium, and tetraethylammonium (Wako Pure Chemical Industries, Ltd., Osaka, Japan). All experiments were carried out at room temperature (20–25°C).

Data analyses

Single-channel currents recorded on the tape were replayed, post-filtered at 0.10 kHz, and digitized at 0.50 ms/point by means of an analog to digital converter (model 2801A, Data Translation Co.). Amplitude of the single-channel currents was measured as a peak-to-peak distance (each peak represents open and closed levels) on the amplitude histogram constructed by a single-channel analysis program, PAT (version 6.2), written by Dr. John Dempster (University of Strathclyde, Glasgow, UK). Single-channel conductance values at a symmetric salt solution were determined by the slope of the current-voltage (*I-V*) curve, where the *I-V* data could be well fitted to a straight line. Single-channel conductance values under asymmetric ionic conditions were obtained by the slope of *I-V* curves at high voltages (≥ 60 mV), where nonlinear *I-V* curves became asymptotic to straight lines. The permeability ratios of the channel (P_{x^+}/P_{K^+}) were defined as

$$P_{x^+}/P_{K^+} = (a_{K^+}/a_{x^+})\exp(VrF/RT) \quad \text{under biionic conditions,} \tag{1.1}$$

$$\frac{P_{Cl^-}}{P_{K^+}} = \frac{[a_{K^+}]_c - [a_{K^+}]_t\exp(-VrF/RT)}{[a_{Cl^-}]_c\exp(-VrF/RT) - [a_{Cl^-}]_t} \quad \text{under asymmetrical conditions,} \tag{1.2}$$

where the reversal potential *Vr* was obtained by fitting the *I-V* curve to the Goldman-Hodgkin-Katz (GHK) voltage equation (Hille, 1992), a_x^+ is the activity of X^+, subscripts *c* and *t* represent *cis* and *trans* sides of the chamber, and other parameters have their usual meanings. Energy profiles for monovalent cations through the channel were obtained by using a program, AJUSTE, written by Alvarez et al. (1992). If available, the activity of each ion was also calculated from the AJUSTE program, in which the effect of the ionic strength of the solution on the activity of each ion is considered.

The ranges of cross-section areas of organic cations were estimated from their CPK (space-filling) models. The CPK models of corresponding cations were drawn and then energy minimized by using the Insight II molecular modeling system. Calculated values are consistent with those reported by others (Coronado and Miller, 1982), which were obtained from silhouette drawings of CPK models of the cations.

RESULTS

Generally, if the AC164 molecules exhibited single-channel behaviors, it appeared a few minutes after the formation of bilayer membranes (see Materials and Methods). The coexistence of several channels, which seemed to behave in an independent manner, was frequently observed. Approximately 10% of the channel could last a few minutes, from which most of the experimental data were obtained. Occasionally, the channel could last over an hour. No voltage-dependent gating behaviors was observed. The mean open time of the channel varied from several to several hundred milliseconds. Despite the variation of gating behaviors of the channel from membrane to membrane, the ion permeation behaviors were stable. Once a channel appeared, most of the time the conductance level was constant at a given voltage. The experiments were therefore focused on the conduction properties of the channel.

Charge selectivity

The charge selectivity of the channel was determined from reversal potentials of *I-V* curves under asymmetric solutions of KCl. The reversal potentials were obtained by fitting current-voltage data to the GHK current equation (Hille, 1992). Permeability ratios (P_{Cl^-}/P_{K^+}) were calculated from the reversal potentials. As shown in Table 1 and Fig. 2, the ratio is ~0.15, indicating that the AC164 channel is a cation-selective channel. According to Table 1, the ratio is almost independent of ionic concentrations, implying that the AC164 channel is a one-ion channel (Levitt, 1986).

I-V relation and monovalent cation selectivity

Fig. 3 *A* shows typical single-channel current traces under a symmetric solution of 500 mM KCl. Neither substate behaviors of conductance nor voltage-dependent gating could be noticed. The *I-V* relationships of the channel shown in Fig. 3 *B* indicate that the current through the open channel

TABLE 1 Charge selectivity (P_{Cl^-}/P_{K^+}) of AC164 channel

Concentration of KCl (*cis/trans* mM)	*Vr* ± SD (mV)	*n*	P_{Cl^-}/P_{K^+}
15/3	−26.8 ± 1.0	3	0.15
20/5	−22.5 ± 2.4	2	0.14
200/50	−23.2 ± 0.6	2	0.13
500/100	−25.4 ± 1.1	3	0.15

Reversal potentials, *Vr*, were obtained according to the procedure described in Fig. 2. Permeability ratios (P_{Cl^-}/P_{K^+}) were calculated in terms of Eq. 1.2.

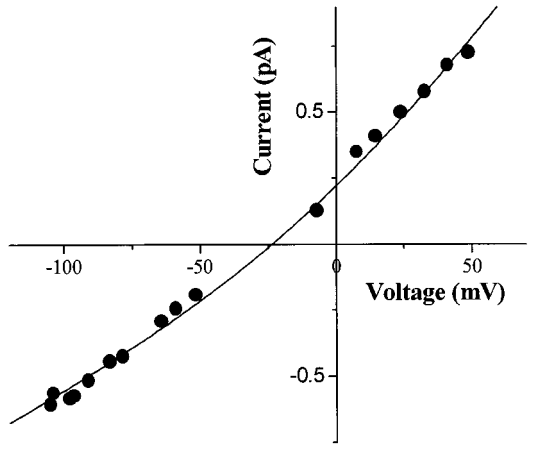

FIGURE 2 *I-V* relationship of the AC164 channel under asymmetrical condition (*cis/trans*, 200/50 mM KCl). Solid line was drawn according to the least-square procedure (Marquardt-Levenberg algorithm) to fit the data to the GHK current equation with the parameters: $Vr = -22.8$ mV and $P_{Cl^-}/P_{K^+} = +0.14$.

is ohmic within a ±150 mV voltage range over an experimental concentration range of 5–500 mM K^+. The channel conductance values reached a maximal value of ~9 pS as ion activities were increased. The conductance-activity relationship nearly followed a simple Michaelis-Menten kinetics with a half-maximal saturating activity, K_m, of ~8 mM and maximal conductance, γ_{max}, of ~9 pS as shown in Fig. 4, suggesting that the channel behaves as if it can be occupied by no more than one ion (at least for K^+ ion) at a time.

The permeability ratios between K^+ and other monovalent cations were measured under biionic conditions by adding a proper amount of K^+ to one side of the membrane and the same amount of another monovalent cation to the opposite side. The selectivity sequence in terms of permeability ratios fell into an order: $NH_4^+ > Cs^+ \geq K^+ > Na^+ \gg Li^+$ (Table 2). Li^+ could neither permeate nor block the channel, suggesting that there is no significant interaction between Li^+ and the channel. The reversal potentials and permeability ratios of Na^+ over K^+ are constant over a wide range of concentrations (10–500 mM; Fig. 5 and Table 2), which is a criterion to demonstrate that the AC164 channel is a one-ion channel (Levitt, 1986). This conclusion is consistent with the chemical compositions of the channel, which does not contain charged or strong polar groups, as electrostatic calculations indicate that a narrow uncharged channel cannot be occupied by more than two ions (Levitt, 1978). To eliminate the influence of anion, gluconate salts of potassium and sodium were used, but no difference from chloride salts was observed within experimental error.

Blockade by Ca^{2+}

No current can be measured on the Ca^{2+} side under biionic conditions of Ca^{2+}/K^+ solutions, suggesting that Ca^{2+} can-

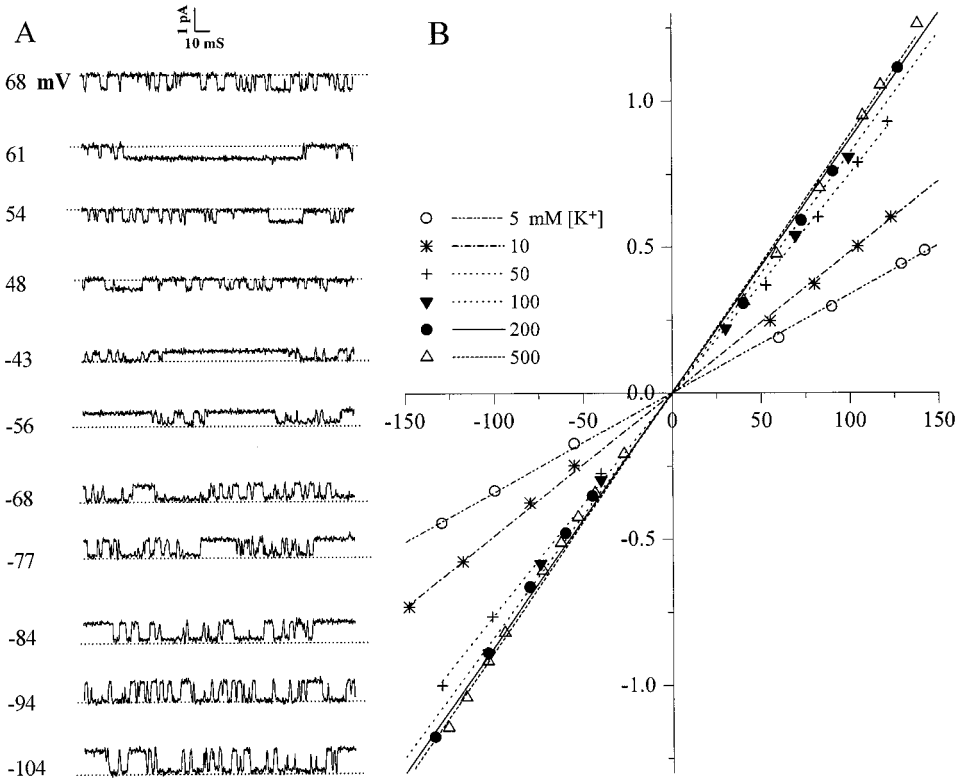

FIGURE 3 Characteristics of the AC164 channel under symmetric K^+ solutions. (*A*) Single-channel current traces under symmetric 500 mM KCl at different voltages. (*B*) Current-voltage relationships of the channel at various concentrations (indicated in *inset*) of symmetric KCl. Each straight line is from a linear regression analysis of the data (*symbols*) obtained from the same membrane.

not permeate through this channel. However, addition of Ca^{2+} to one side of the chamber containing symmetrical KCl solutions caused apparent reductions of the single-channel currents (Fig. 6 *A*). Relative currents (I/I_0) could be fitted with a single-site titration curve according to

$$I/I_0 = \{(1 + [Ca^{2+}]/K_d(V))\}^{-1}, \quad (2)$$

where $K_d(V)$ is the dissociation constant at a given voltage V, $[Ca^{2+}]$ is the concentration of Ca^{2+} in the solution, and I and I_0 are the currents at a given voltage with or without Ca^{2+}. As shown in Fig. 6 *B*, the data are well fitted to an inhibition curve with K_d (+100 mV) of 0.6 mM for Ca^{2+}. This suggests that the Ca^{2+} interacts with the channel in a one-to-one fashion. The blockade of the channel by Ca^{2+} was in a dose- and voltage-dependent manner. The current was inhibited more strongly as the membrane voltage increased when Ca^{2+} was added to the *cis* side (Fig. 6 *C*). By assuming that the inhibition is due to the competition for a binding site located at the electrical distance of $z\delta$ from the *cis* entrance of the channel, relative conductance values (γ/γ_0) could be described as

$$\gamma/\gamma_0 = \{1 + [Ca^{2+}]/K_d(0)\exp(z\delta FV/RT)\}^{-1}, \quad (3)$$

according to Woodhull's blocking theory (Woodhull, 1973), where $K_d(0)$ is an apparent zero voltage dissociation con-

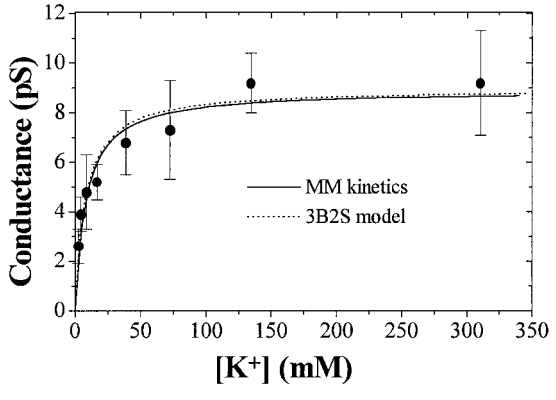

FIGURE 4 Conductance-activity relationship of the AC164 channel. Each value, which was obtained from at least three different membranes, represents the mean ± SD. The solid line was drawn according to the same method in Fig. 2 to fit the data to the Michaelis-Menten (MM) kinetics with the parameters $\gamma_{max(K^+)}$ = 8.9 pS and $K_{m(K^+)}$ = 8.3 mM, whereas the dotted line was drawn according to the 3B2S model with the parameters for K^+ listed in Table 3.

TABLE 2 Cation selectivity (P_{X^+}/P_{K^+}) of AC164 channel under various biionic conditions

Concentration	(*cis*/*trans* mM)	*Vr* ± SD (mV)	*n*	P_{X^+}/P_{K^+}
10	(K^+/Na^+)	−24.7 ± 1.6	4	0.39
50	(K^+/Na^+)	−22.4 ± 1.9	5	0.42
100	(K^+/Na^+)	−23.5 ± 1.1	3	0.40
500	(K^+/Na^+)	−22.1 ± 0.8	3	0.40
500	(K^+/Cs^+)	1.7 ± 2.7	3	1.06
500	(K^+/NH_4^+)	8.2 ± 1.9	3	1.37
50	(K^+/Li^+)	−∞	6	0
500	(K^+/Li^+)	−∞	5	0

Reversal potentials, *Vr*, were obtained from the same procedure described in Fig. 5. Permeability ratios were calculated in terms of Eq. 1.1.

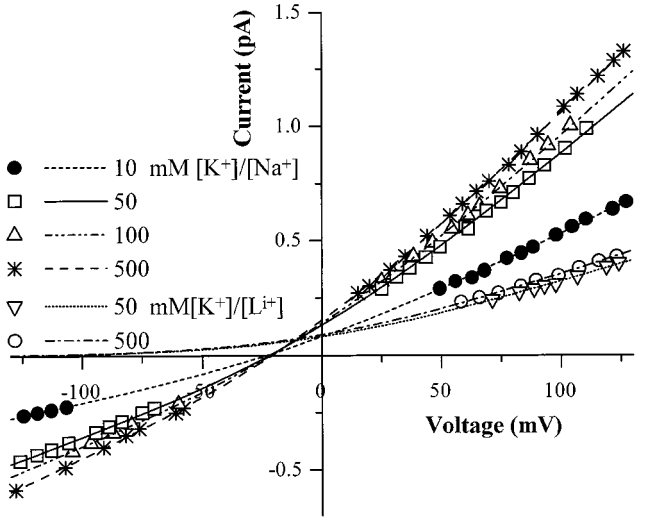

FIGURE 5 Single-channel current-voltage relationships of the AC164 channel under various biionic conditions. Each curve was drawn according to the same procedure in Fig. 2 to fit the experimental data that were obtained from same membrane. The best-fit reversal potentials for K^+/Na^+ solutions are listed in Table 2, and those for K^+/Li^+ solutions were estimated to be minus infinite value ($-\infty$).

stant for Ca^{2+}. The values of $z\delta$ and $K_d(0)$ estimated from the best fit to the experimental data at a Ca^{2+} concentration of 0.5 mM (reverse triangles and solid line in Fig. 6 *C*) were 0.07 and 0.81 mM (Fig. 6 *D*). Moreover, nearly the same values were obtained when Ca^{2+} was added to the *trans* side of the chamber, indicating that the channel has two symmetrical binding sites, each of which is located in the vicinity of each channel entrance. By assuming that K^+ and other monovalent cations bind at the same position (see Discussion), the value of $z\delta$ for monovalent ions should be one-half of that for Ca^{2+} due to the bearing of two charges by Ca^{2+}. This means that the electrical distance of the binding site for the permeant monovalent ions is symmetrically located at a 3.5% voltage drop from each entrance of the channel. This result gives additional evidence that the channel has a symmetrical structure.

Estimation of the pore size

Ammonium-derivative organic cations have been used to probe the atomic dimension of the pore size of ion channels for a long time (Hille, 1971; Coronado and Miller, 1982). Here, we used the same method to estimate the pore size of the AC164 channel. As Cl^- has no observed effect on the channel conductance (see the section of *I-V* relation and monovalent cation selectivity), 500 mM KCl was applied in one side of the chamber to make sure the channel is first formed by measuring K^+ current, and then the voltage was shifted to the other side containing 500 mM organic cation to check the current. If no detectable current (less than 0.1 pA) was observed at a voltage higher than ± 150 mV, we determine that the organic cation cannot permeate through the channel. Among the organic cations tested, the largest conductance was demonstrated by ammonium ion ($\sim$10 pS), and substitution of a single -H by $-CH_3$ (monomethylammonium) produced substantial reduction in the channel conductance ($\sim$3 pS). This is probably due to the fact that, unlike NH_4^+, methyl groups cannot participate in hydrogen bonding with its immediate environment (Coronado and Miller, 1982). In the case of larger cations, no current fluctuations at all could be discerned. These nonpermeant cations included monoethylammonium, aminoguanidinium, diethylammonium, choline, tetramethylammonium (TMA), and tetramethylammonium (TEA). These results were confirmed with symmetric solutions for all of the salts.

In Fig. 7, these conductance values are plotted against the cross-section areas of the cations. The largest ion that can permeate through the channel is monomethylammonium (Fig. 1 *B*). No channel conductance values could be measured for cations with cross-section areas larger than that of monoethylammonium (Fig. 1 *C*). These nonpermeant cations included planar shaped molecules such as guanidine derivatives, symmetrical quaternary amines, and large primary, secondary, and tertiary amines. Moreover, almost no reduction of single-channel currents could be observed by adding these nonpermeant cations (up to 1 mM) into symmetrical solutions containing KCl salt, indicating that there is no interaction between these nonpermeant cations and the channel molecule. Thus, it is likely that these molecules were excluded solely on the basis of size, rather than by specific interactions with the channel. Therefore, we postulate that the narrowest constriction of the channel is between 22 and 27 $Å^2$ in area by assuming that the nonhydrated size of these cations is the important parameter. As a result, the diameter of the narrowest portion of the channel should be $\sim$6 Å, slightly less than that of the nAChR channel (Karlin and Akabas, 1995).

DISCUSSION

Correlating structure and function of a channel is essential for understanding the underlying physicochemical basis involved in channel behaviors. The present study clearly demonstrates that the AC164 channel is a one-ion channel with monovalent cation selectivity. In the following, energy profiles for ion permeation through the channel are built according to the 3B2S model of Eyring's theory. A structural model of the channel is constructed according to lines of available structural information, and correlations of the structure and function of the channel are discussed.

3B2S model

With a symmetrical structure spanning across the membrane, an unoccupied AC164 channel should have a symmetrical energy profile for ions at 0 mV. The Michaelis-Menten kinetics of K^+ permeation through the channel (Fig. 4) and the constant permeability ratio of Na^+ over K^+ (Table 2) strongly suggest that the AC164 channel is a

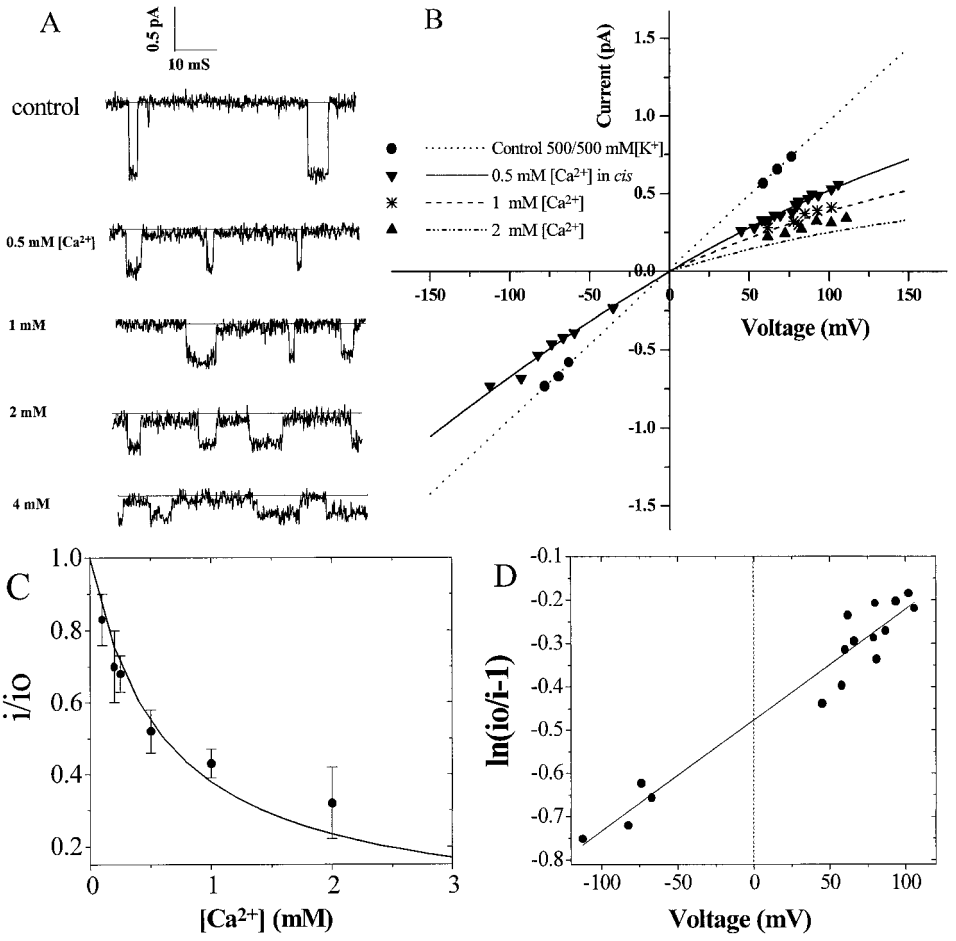

FIGURE 6 Voltage-dependent blockade by Ca^{2+}. (*A*) Single-channel current trances at +100 mV in the presence of various concentrations of *cis* Ca^{2+}. (*B*) Dose-dependent inhibition curve. Relative single-channel currents (*I*/*Io*) against the concentrations of *cis* Ca^{2+} at +100 mV. Each set of data, which were taken from at least three different membranes, represent the mean ± SD. The solid line was the best fit to Eq. 2 with $K_{d(+100\ mV)}$ = 0.61 mM according to the same procedure in Fig. 2. (*C*) Current-voltage relationships in the presence of various concentrations of *cis* Ca^{2+}. Lines were drawn according to GHK current equation. (*D*) Linearized plot of the data in *C* at Ca^{2+} concentration of 0.5 mM. The straight line is from a linear regression analysis of the data according to Eq. 3 with the blocking parameters $z\delta$ = 0.07 and $K_{d(0\ mV)}$ = 0.81 mM.

one-ion channel. The voltage-dependent blocking effect of Ca^{2+} on the single-channel current indicated that the channel has two accessible binding sites. In addition, based on the formula constructed by Chang et al. (1994), an upper limit for the surface charge density σ_{max} can be expressed as

$$\sigma_{max} < \{K_m\gamma_{int}/(\gamma_{max} - \gamma_{int})\}^{1/2}/272, \quad (4)$$

where the unit of σ_{max} and dissociation constant K_m are given in electron charges/Å^2 and moles/liter, and γ_{int} is the intersection with the ordinate axis of the straight-line tangent to the activity-conductance curve at any point, but with the best estimation at the point corresponding to the lowest conductance experimentally available. Drawing the tangent to the curve in Fig. 4 from the point at the lowest concentration used in the experiments (3 mM), we get γ_{int} = 0.8 pS. Applying Eq. 4 we can estimate that σ_{max} is less than 0.0001 electron charges/Å^2. This small charge density would be effectively screened by the ion concentrations used in the experiments. The small value for the upper limit of the charge density is in good agreement with the chemical compositions of the channel, which does not contain charged or strong polar groups. In contrast, this value is much smaller than the asolectin membrane surface charge density (Bell and Miller, 1984). However, if the entrance of the channel projects into the bulk solution, it will shield the channel from the influence of the membrane surface charge as indicated by Jordan (1986). This inference is consistent with our experiments on charge selectivity of the channel.

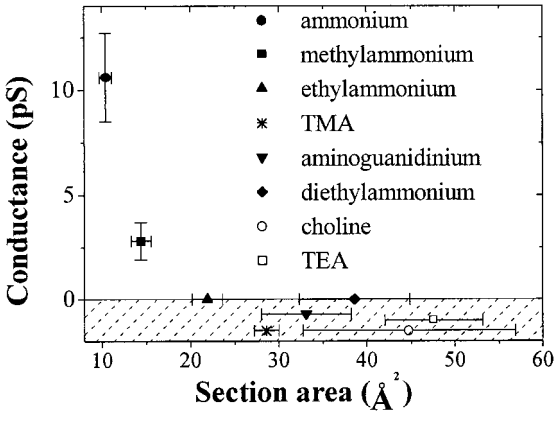

FIGURE 7 Channel conductance values versus cross-section areas of organic cations. Cross-section areas were measured from CPK models of the organic cations by using an Insight II molecular modeling program (Biosym/MSI, San Diego, CA). The horizontal bars on the symbols indicate the range between smallest and largest cross-section area of the organic cations. The symbols and vertical bars represent the mean ± SD of conductance values that were taken from at least three different membranes. The broken slashed area indicates an expanded zero current range to show the data more clearly.

According to Gouy-Chapman theory, if negative surface charges are presented in the vicinity of the channel entrance, it will increase the ionic strength of the cation in the vicinity of the channel entrance more at low salt concentration than at high salt concentration. Therefore, the constant of the charge selectivity (P_{Cl^-}/P_{K^+}) of the channel under various asymmetrical conditions (Table 1) suggested that the surface charge should have little effect on the channel behaviors. Moreover, unlike Bell and Miller's result, the concentration-activity relationship of the AC164 channel followed simple Michaelis-Menten kinetics from a low concentration of 3 mM K^+ to a high concentration of 500 mM K^+. It is this result that directly led us to estimate the upper limit of the surface charge density.

The above results strongly argue that a three-energy-barrier two-binding-site (3B2S) model of Eyring rate theory with one-ion occupancy (one-ion channel), a symmetrical energy profile, and no surface charge is suitable for the energy profiles of permeant ions. Therefore, this model was used to fit sets of experimental data under different ionic conditions simultaneously. These data include *I-V* data at both symmetrical (5, 10, 50, 100, 200, and 500 mM [K^+]) and biionic (10, 50, 100, and 500 mM [K^+/Na^+] as well as 50 and 500 mM [K^+/Li^+]) conditions according to Alvarez et al. (1992). By unresolved origin, the standard deviation (SD) of the channel conductance is relatively large as shown in Fig. 4. Therefore, *I-V* data from at least three different membranes under the same ionic condition were adjusted to their average value to fit the 3B2S model. The values for electrical distances of energy barriers and energy wells were not pre-set but were adjusted gradually as long as the symmetrical energy profile was ensured. Optimization of the parameters underwent several steps. First, energetic parameters (energy values at peaks G1, G2, and G3 and wells U1 and U2) for each ion were varied with fixed symmetrical distance parameters. Next, the distance parameters and energetic parameters were optimized simultaneously. Then, the distance parameters (D1, D2, D3, D4, D5, L1, and L2) were fixed at new values, and the energetic parameters were reoptimized. These steps were repeated several times until the SUMSQ, the weighted sum of squared differences of experimental and theoretical data, was minimized. The final results are shown in Table 3 and Fig. 8. The electric distance of the binding site, D = D1 + D2, is 0.054 for monovalent cations. This value is nicely in agreement with the value of 0.035, which was estimated from the Ca^{2+}-blocking experiment by assuming that these ions share the same binding sites.

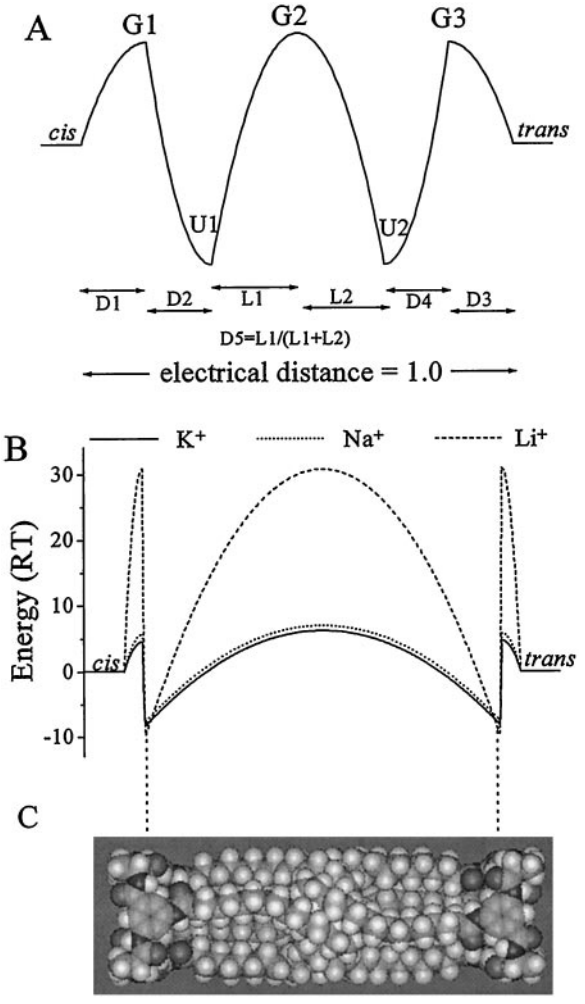

FIGURE 8 Best-fit energy barrier profiles for K^+, Na^+, and Li^+ permeation through the AC164 channel. (*A*) Schematic diagram of the 3B2S model parameters. The peak energies G1, G2, and G3 and well energies U1 and U2 are referred to the energy level of the *cis* and *trans* solutions in units of RT with their positions defined as D1–D5. (*B*) Best-fit energy profiles for K^+, Na^+, and Li^+ at 0 mV. Lines are drawn according to the energy parameters listed in Table 3 and the distance parameters D1 = D3 = 0.047, D2 = D4 = 0.007, and D5 = 0.5. (*C*) CPK model of a side view of the AC164 channel. Double arrows indicate the most probable locations of the binding sites that correspond to energy wells.

TABLE 3 Best-fit energy profile parameters of the 3B2S model for Na^+, Li^+, and K^+

Parameter	K^+ (RT)	Na^+ (RT)	Li^+ (RT)
G1	4.57 ± 0.01	5.68 ± 0.08	30.90 ± 0.01
G1	6.18 ± 0.01	6.95 ± 0.13	30.77 ± 0.26
G3	4.57 ± 0.01	5.68 ± 0.08	30.90 ± 0.01
U1	−8.19 ± 0.01	−7.59 ± 0.05	−9.63 ± 0.01
U2	−8.19 ± 0.01	−7.59 ± 0.05	−9.63 ± 0.01

The fitting routine was described in the text. Final values of distance parameters obtained from the routine are D1 = D3 = 0.047, D2 = D4 = 0.007, and D5 = 0.5. The minimized value of the weighted sum of squared differences of experimental and theoretical data, SUMSQ, is 2.93.

Structural model

In this section, we are trying to construct a structural model of the channel by combining several lines of independent structural information. First, the AC164 molecule has an inherent four-fold rotationally symmetrical structure composed of a head formed of a cyclic octa-peptide ring and acyl chain tails. The symmetrical and rigid structure of the peptide ring has been confirmed by NMR data of the pep-

tide in DMF-d7 solution, which shows that the symmetrical structure of the peptide ring remains in the range of temperature from −50 to 100°C (Donowaki et al., 1996). And the connection of acyl chains on Aba residues of the ring was ensured by the synthetic process (see Materials and Methods). Second, the overall structure of the channel has been explored with present electrophysiological experiments. The symmetrical *I-V* relationship (Fig. 3 *B*) and the symmetrical binding sites obtained by the Ca^{2+}-blocking experiment suggested that the channel has a symmetrical structure spanning across the lipid bilayer membrane. Third, estimation of the pore size with a set of organic cations implied that the diameter of the narrowest portion of the channel pore is ~6 Å. Finally, according to the primary structure of a single AC164 molecule, all the hydrophilic groups, no matter whether they are from the electron-rich π-faces of the benzoic rings and Aba residues or from the carbonyl groups of both Ala and Aba residues, are on the peptide ring. On the other hand, the results from the Ca^{2+} blockade of the channel has indicated that two binding sites are located symmetrically in each vicinity of the channel entrance. Combining these two facts, it is highly likely that the peptide ring provides the binding site to ions and is located in the vicinity of the channel entrance, as it is the only hydrophilic part of the molecule. This inference is consistent with a molecular dynamics simulation of water permeation through the channel, where it has been demonstrated that the hydrophilic environment of the peptide ring gives an energy well for the water (Qi and Sokabe, 1998). From the above information, the AC164 channel should have a symmetrical structure spanning across the membrane via a tail-to-tail associated dimer with the peptide ring located in the vicinity of the channel entrance and with a pore of 6 Å in width.

There are several possible ways for the formation of a channel from the AC164 molecule(s) to occur. First, the channel is formed from a single molecule. This is impossible, as a single molecule is not long enough to span the bilayer. Second, the channel is formed from an association of many molecules. This possibility may be eliminated, because no substate of conductance values can be noticed in single-channel current traces (Fig. 3 *A*). If molecular aggregation happens, substate conductance values would likely be observed due to the different number of molecular aggregations (Kobuke et al., 1992). Third, in terms of energetics, the hydrophilic peptide ring is not likely to be buried in the core of the lipid membrane, i.e., the channel would not formed from a head-to-head associated dimer of the molecule. This consideration is supported by our inference from the Ca^{2+}-blocking experiment that the peptide ring is located in the vicinity of the channel entrance. Fourth, the channel is formed from a stack of rings across the membrane. However, due to the poor solubility of the AC164 in lipid solution, we never observed the appearance of the channel by adding the AC164 just on one side of the membrane. This fact suggests that the AC164 molecule cannot readily cross the membrane and implies that the AC164 channel is not formed from the stack of the rings. In addition, data from ^{1}H-NMR showed that the purity of the AC164 molecule is over 99%. And the channel has been observed in a concentration of AC164 as low as 1 μM. These facts might suggest that the channel does not originate from trace impurities. Therefore, the only way to form the AC164 channel is through a tail-to-tail associated dimer of the molecule. This idea can be tested in principle by measuring the concentration dependence of channel formation probability. However, this is virtually impossible, because of the poor solubility of AC164 in lipid solution and the difficulty of estimating how many molecules moved into the lipid solution in our method (see Materials and Methods). Finally, it is worthy to mention our earlier abstract (Sokabe et al., 1996), where we reported that for molecules with three, four, or five dipeptide repeats in the ring, no significant difference among different peptides was observed. This is a surprising result, as it is generally thought that the larger the diameter of the entrance, the larger the conductance of the channel. However, from the view of biophysics, the situation is not so simple. It is recognized that, whatever structures are involved, the ion permeation properties are determined by the interaction of an ion with its surrounding environment (Chen and Eisenberg, 1993). For example, even though Li^+ has the smallest radius among all ions, it cannot permeate across most ion channels due to its strong interaction with surrounding water molecules. Enlargement of the ring size of these channel-forming peptides might increase the probability of ion entering. But, on the other hand, the enlargement will weaken the interaction between the ion and the binding site, which is most likely provided by the ring of the peptides, at the same time. Based on experimental results that all channels have similar conduction properties, we argue that the process of an ion passing through the hydrophobic acyl chain pore, which is shared by all of these channel-forming peptides, is the rate-limiting step for ion permeation through all of these channels.

In summary, the AC164 channel should be formed by a tail-to-tail associated dimer of the molecule with the hydrophobic acyl chains lining the pore and the hydrophilic peptide ring forming the entrance of the channel. This structural model is supported by an optimized conformation of an AC164 monomer (Fig. 1 *D*) (Qi and Sokabe, 1998), the pore diameter of which is ~6 Å, just about the same size as that of the channel formed from a dimer of the molecule. Molecular dynamics simulation of water permeation through this structure of the channel, where a physically reasonable diffusion process and energy barriers of water permeation through the channel have been demonstrated (Qi and Sokabe, 1998), suggested that this structure is physicochemically possible as an ion channel. Furthermore, this structural model is also supported by recent findings that a certain class of lipid molecules (Sokabe, 1984; Hayashi et al., 1978), *de novo* synthesized nonpeptide molecules (Tanaka et al., 1995; Pregel et al., 1995) and nonpolar peptide molecules (Oliver and Deamer, 1994) can

form ion channels, the pores of which were supposed to be lined with relatively hydrophobic groups.

Based on this simple structural model the structure and function of the channel could be correlated. The peptide ring, with its rigid structure (Ishida et al., 1997) on one hand, provides a cavity for the entering of water and permeant ions into the pore and, with its hydrophilic feature on the other hand, forms the channel entrance at the membrane-water interface and gives the binding site for ions. Consequently, the acyl chains line across the membrane form an ion-conducting pathway. These correlations can be made more concrete with the aid of the analysis using the 3B2S model. The energy peaks near the entrance might arise from the dehydration energy, which is inversely related to the ionic radius (Hille, 1992), for at least stripping the outer shell of water surrounding the ion. The electron-rich π-faces of aromatic rings may be responsible for the cation selectivity of the channel (Tanaka et al., 1995) and provide the binding site, i.e., the energy well of the 3B2S model for permeant ions. Lacking of strong polar or charged groups to attract ions, the access of ions to the interior of the channel is dominated by the dehydration energies (Hille, 1992). Cs^+ would then be the most favored among alkali metal cations, as it is most easily dehydrated. This might be responsible for the selectivity order of $Cs^+ \geq K^+ > Na^+ \gg Li^+$.

The acyl chains spanning across the membrane might be responsible for the width and height of the central barrier of the 3B2S model. However, the idea that the acyl chains span across the membrane to provide a pathway for ion permeation challenges the conventional belief that the channel should be lined with polar or charged residues (Hille, 1992). A partial reason to account for this might come from the study on the hydration of alkali ions in the gas phase (Dzidic and Kebarle, 1970). This study has shown that hydration of an ion is not an additive function of the number of water molecules. Approximately 20% or 36% of bulk phase hydration energy is attained when the first or first two water molecules bind to the ion; when four water molecules have bound, the aggregate interaction energy is 50% of the bulk hydration energy. Therefore, it is reasonable that an ion is stabilized by at least four to six intrapore water molecules surrounding the ion when it permeates across the hydrophobic pore of the channel due to its relatively large pore.

CONCLUSIONS

To explore the structure and function of the AC164 channel, systematic electrophysiological analyses on the ion conduction properties and structure aspects of the channel have been performed. Single-channel recordings have demonstrated that the channel can mimic typical single-channel features, including open-closed fluctuations, stable conductance, ion selectivity, conductance saturation at high salt concentrations, and voltage-dependent blockade by Ca^{2+}. Structural information strongly suggests that the channel is formed from a tail-to-tail associated dimer of the molecule. This structural model is supported by several lines of independent evidence. They include the primary structural information of a monomer, i.e., the inherent four-fold rotationally symmetrical structure of a single AC164 molecule and structural model created via simulated annealing and restrained molecular dynamics (Qi and Sokabe, 1998). They also include direct structural information obtained from present electrophysiological experiments and indirect structural information, i.e., the consistency between the energy profile, for permeant ions in this study obtained from 3B2S model and that for water molecules in a previous study (Qi and Sokabe, 1998).

Through this study, we have constructed a suitable channel structure that can correlate with its functions. Based on the simple structure, we are going to explain the channel function by performing molecular dynamics simulation on ion permeation. Recently, several pieces of evidence have appeared to support a notion that the pore of natural ion channels, including AChR channels, might be lined with nonpolar residues (Andersen and Koeppe, 1992). Thus, the AC164 channel provides a good model to study how an ion can permeate through hydrophobic pore regions of natural ion channels.

We thank Ms. Q. Y. Tang for doing the test experiment at a low concentration of the AC164 molecule.

This work was partly supported by grants from the Science and Technology Agency of Japan, Japan Society for Promotion of Science (to M. Sokabe), and Naito Memorial Science Foundation (to H. Ishida).

REFERENCES

Alvarez, O., A. Villarroel, and G. Eisenman. 1992. Calculation of ion currents from energy profiles and energy profiles from ion currents in multibarrier, multisite, multioccupancy channel model. *Methods Enzymol.* 207:816–854.

Andersen, O. S., and R. E. Koeppe II. 1992. Molecular determinants of channel function. *Physiol. Rev.* 72:S89–S158.

Bell J. E., and C. Miller. 1984. Effect of phospholipid surface charge on ion conduction in the K^+ channel of sarcoplasmic reticulum. *Biophys. J.* 45:279–287.

Chang, H., S. Ciani, and Y. Kidokoro. 1994. Ion permeation properties of the glutamate receptor channel in cultured embryonic *Drosophila* myotubes. *J. Physiol.* 476:1–16.

Chen, D. P., and R. S. Eisenberg. 1993. Flux, coupling, and selectivity in ionic channels of one conformation. *Biophys. J.* 65:727–746.

Coronado, R., and C. Miller. 1982. Conduction and block by organic cations in a K^+-selective channel from sarcoplasmic reticulum incorporated into planar phospholipid bilayers. *J. Gen. Physiol.* 79:529–547.

Donowaki, K., K. Ohkubo, and H. Ishida. 1996. Molecular design and synthesis of functional peptides which include a non-natural amino acid. *Peptide Chem.* 413–416.

Dzidic, I., and P. Kebarle. 1970. Hydration of alkali ions in the gas phase: enthalpies and entropies of reactions $M^+(H_2O)_{n-1} + H_2O = M^+(H_2O)_n$. *J. Phys. Chem.* 74:1466–1474.

Egberts, E., S. J. Marrink, and H. J. C. Berendsen. 1994. Molecular dynamics simulation of a phospholipid membrane. *Eur. Biophys. J.* 22:423–436.

Hayashi, F., M. Sokabe, M. Takagi, K. Hayashi, and U. Kishimoto. 1978. Calcium-sensitive univalent cation channel formed by lysotriphosphoinositide in planar bilayer lipid membranes. *Biochim. Biophys. Acta.* 510:305–315.

Heginbotham, L., and R. MacKinnon. 1992. The aromatic binding site for tetraethylammonium ion on potassium channels. *Neuron.* 8:483–491.

Hille, B. 1971. The permeability of the sodium channel to organic cations in myelinated nerve. *J. Gen. Physiol.* 58:599–619.

Hille, B. 1992. Ionic channels of excitable membranes, 2nd ed. Sunderland, MA, Sinauer.

Ishida, H., K. Donowaki, Y. Inoue, Z. Qi, and M. Sokabe. 1997. Synthesis and ion channel formation of novel cyclic peptides that include a non-natural amino acid. *Chem. Lett.* 935–954.

Jordan, P. C. 1986. Ion channel electrostatics and the shapes of channel proteins. *In* Ion Channel Reconstitution. C. Miller, editor. Plenum Press, New York. 37–55.

Jordan, P. C. 1990. Ion-water and ion-polypeptide correlations in a gramicidin-like channel: a molecular dynamics study. *Biophys. J.* 58: 1133–1156.

Karlin, A., and M. H. Akabas. 1995. Toward a structural basis for the function of nicotinic acetylcholine receptors and their cousins. *Neuron.* 15:1231–1244.

Kobuke, Y., K. Ueda, and M. Sokabe. 1992. Artificial non-peptide single ion channels. *J. Am. Chem. Soc.* 114:7618–7622.

Kumpf, R. A., and D. A. Dougherty. 1993. A mechanism for ion selectivity in potassium channels: computational studies of cation-π interactions. *Science.* 261:1708–1710.

Lear, J. D., Z. R. Wasserman, and W. F. DeGrado. 1988. Synthetic amphiphilic peptide models for protein ion channels. *Science.* 240: 1177–1181.

Levitt, D. G. 1978. Electrostatic calculations for an ion channel. I. Energy and potential profiles and interaction between ions. *Biophys. J.* 22: 209–219.

Levitt, D. G. 1986. Interpretation of biological ion channel flux data: reaction-rate versus continuum theory. *Annu. Rev. Biophys. Biophys. Chem.* 15:29–57.

Miller, C. 1993. Potassium selectivity in proteins: oxygen cage or π in the face? *Science.* 261:1692–1693.

Nomura, K., K. Naruse, K. Watanabe, and M. Sokabe. 1990. Aminoglycoside blockade of Ca^{2+}-activated K^+ channel from rat brain synaptosomal membranes incorporated into planar bilayers. *J. Membr. Biol.* 115:241–251.

Oiki, S., W. Danho, V. Madison, and M. Montal. 1988a. M2 delta, a candidate for the structure lining the ionic channel of the nicotinic cholinergic receptor. *Proc. Natl. Acad. Sci. U.S.A.* 85:8703–8707.

Oiki, S., W. Danho, and M. Montal. 1988b. Channel protein engineering: synthetic 22-mer peptide from the primary structure of the voltage-sensitive sodium channel forms ionic channels in lipid bilayers. *Proc. Natl. Acad. Sci. U.S.A.* 85:2393–2397.

Oliver, A. E., and D. W. Deamer. 1994. α-Helical hydrophobic polypeptides form proton-selective channels in lipid bilayers. *Biophys. J.* 66: 1364–1379.

Pregel, M. J., L. Jullien, J. Canceill, L. Lacombe, and J. M. Lehn. 1995. Channel-type molecular structures. IV. Transmembrane transport of alkali-metal ions by 'bouquet' molecules. *J. Chem. Soc.* 2:417–426.

Qi, Z., and M. Sokabe. 1998. Dynamic properties of individual water molecules in a hydrophobic pore lined with acyl chains: a molecular dynamics study. *Biophys. Chem.* 71:35–50.

Roux, B., and M. Karplus. 1994. Molecular dynamics simulations of the gramicidin channel. *Annu. Rev. Biophys. Biomol. Struct.* 23:731–761.

Sokabe, M. 1984. Aminoglycoside blockade of cation channels from polyphopsphoinositides and sarcoplasmic reticulum in planar bilayer lipid membranes. *In* Transmembrane Signaling and Sensation. F. Oosawa, H. Hayashi, and T. Yoshioka, editors. JSSP/VNU Science Press, Tokyo. 119–134.

Sokabe, M., A. Auerbach, and F. J. Sigworth (editors). 1997. Progress in Cell Research, Vol. 6: Towards Molecular Biophysics of Ion Channels. Elsevier Science, Amsterdam.

Sokabe, M., M. Kasai, K. Nomura, and K. Naruse. 1991. Electrophysiological analysis of structural aspects of voltage-dependent SR K^+ channel. *Comp. Biochem. Physiol.* 98C:23–30.

Sokabe, M., Z. Qi, H. Ishida, and K. Donowaki. 1996. Ion channels formed from cyclic peptides with acyl chains. *Biophys. J.* 70:A201.

Tanaka, Y., Y. Kobuke, and M. Sokabe. 1995. Non-peptide ion channel with a K^+-selective filter. *Angew. Chem. Int. Edit.* 34:693–694.

Tempel, B. L., D. M. Papazian, T. L. Schwarz, Y. N. Jan, and L. Y. Jan. 1987. Sequence of a probable potassium channel component encoded at Shaker locus of *Drosophila*. *Science.* 237:770–775.

Woodhull, A. M. 1973. Ionic blockage of sodium channels in nerve. *J. Gen. Physiol.* 61:687–708.